ACS Catalysis

Letter

pubs.acs.org/acscatalysis

CO Oxidation by Subnanometer Ag_xAu_{3-x} Supported Clusters via Density Functional Theory Simulations

F. R. Negreiros,[†] L. Sementa,[†] G. Barcaro,[†] S. Vajda,[‡] E. Aprá,[§] and A. Fortunelli*[,†]

[†]CNR-IPCF, Istituto per i Processi Chimico-Fisici del Consiglio Nazionale delle Ricerche, Pisa 56124, Italy

[‡]Materials Science Division, Center for Nanoscale Materials, Argonne National Laboratory, Argonne, Illinois 60439, United States and Department of Chemical and Environmental Engineering, Yale University, New Haven, Connecticut 06520, United States

[§]William R. Wiley Environmental Molecular Science Laboratory, Pacific Northwest National Laboratory, Washington 99352, United States

Supporting Information

ABSTRACT: The activity of Ag_xAu_{3-x}/MgO(100) clusters in CO oxidation is investigated computationally via systematic sampling techniques. It is found that these subnanometer species transform after ligand adsorption into reaction complexes which catalyze CO oxidation through a variety of different mechanisms, occurring via both Langmuir−Hinshelwood and Eley−Rideal paths and in some cases directly involving the oxide support. The alloyed Ag_2Au_1 cluster is proposed as the best catalyst in terms of efficiency and robustness.

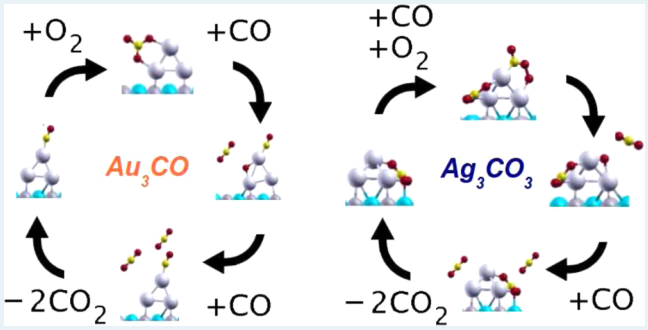

KEYWORDS: *ultrananoclusters, heterogeneous catalysis, catalyst stability, nanocatalysis, alloyed clusters*

Oxidation of carbon monoxide to dioxide ($2CO + O_2 = 2CO_2$) is an environmentally important process in the present carbon-based energy cycle, and as such has been intensively studied in recent years at both the experimental and the theoretical level.[1,2] From a thermodynamic point of view, the process is strongly exothermic with a reaction enthalpy of 5.86 eV. However, the stability of the carbon lone pair in CO and of the O_2 bond makes it a very slow process in ambient conditions. A catalyst is thus needed which can efficiently adsorb one or both reactants and significantly lower the reaction energy barriers. The catalyst should also be sufficiently robust at realistic pressures of O_2 and CO to avoid sintering and catalyst deactivation.

Commercially used catalysts, for example, in exhaust-gas treatment are based on Pd, Pt, or Rh particles (pure or alloyed) on properly prepared oxide substrates. However, after Haruta's discovery that supported gold nanoclusters are active in CO oxidation at low temperature,[3,4] a wealth of studies has flourished on this topic, see, for example, refs 5−13 A crucial result is experimental evidence that the real actors of CO oxidation can be subnanometer species containing ∼10 Au atoms.[14] This finding contributed to trigger studies on heterogeneous catalysis by extremely small (subnanometer) metal clusters, a somewhat novel and fascinating field,[15−18] although older suggestions of its importance had been advanced[19] based on EXAFS data.[20] On the theoretical side, heterogeneous subnanocatalysis offers exciting perspectives, as the small size of the clusters allows for detailed and accurate studies involving all possible products from a specific reaction as well as all possible paths connecting them (including the possible effect of the cluster/support interface), thus achieving a complete description of the process.[21]

In terms of size dependence, it is known that supported Au atoms and dimers are not able to coadsorb CO and O_2 molecules, and are so unable to catalyze their reaction,[22,23] in analogy to compact surfaces. Therefore, there must be a minimum and an optimal cluster size, but these issues have not been investigated in depth so far.[7] Moreover, although many studies of pure free and supported metal catalyst can be found in the literature, the same cannot be said of the alloyed case, where previous work has been mostly focused on ligand adsorption and reaction on (usually charged) gas-phase species.[24−27] If one considers that Ag anions promote CO oxidation in the gas-phase[28] and Au_6[17] and Ag_3[18] supported clusters are effective alkene oxidation catalysts, while large Ag−Au mixed particles[29] and nanoporous mixed systems[30] have been shown to be better CO oxidation catalysts than pure gold ones, it is both natural and promising to investigate the effect of Ag−Au alloying at the subnanometer scale.

In the present work, we address these questions by assessing the performance of Ag_xAu_{3-x} trimers supported on the MgO(100) surface as catalysts in CO oxidation. Calculations

Received: April 28, 2012
Revised: July 11, 2012
Published: July 23, 2012

are performed using a GGA xc-functional[31] and a plane-wave basis set within a periodic approach.[32] The MgO(100) surface is selected as a reasonable model of an ionic support, as shown in a recent study by comparison with amorphous alumina.[21] A systematic exploration of the potential energy surface (PES) of the metal-cluster + substrate + ligands system is conducted via a reactive global optimization approach[21] (see the Supporting Information), to determine the catalytic cycle and the robustness of the catalysts. It is found that trimers are the smallest supported clusters able to act as effective CO oxidation catalysts in complex cycles occurring via Langmuir−Hinshelwood or Eley−Rideal mechanisms. The effect of the cluster/oxide interface is taken into account and analyzed. It is shown that mixing two different metals can have beneficial effects on the catalytic activity as well as on the stability (resistance to sintering) of these subnanometer species.

In the Supporting Information, we report representative structures of bare M_3 (i.e., Ag_xAu_{3-x}) trimer clusters, as well of their complexes with O_2 and CO molecules. Molecular adsorption energies of one or two O_2 or CO molecules are reported in Table 1. The lowest-energy configurations of bare

Table 1. Molecular Adsorption Energies[a] on Ag_xAu_{3-x} and $Ag_xAu_{3-x}O$ Clusters[b]

		$x = 0$	$x = 1$	$x = 2$	$x = 3$
Ag_xAu_{3-x}	O_2	1.01	1.11	1.16	1.19
	$2O_2$	1.01	1.11	1.57	1.62
	CO	1.34	1.26	0.85	0.81
	2 CO	1.71	1.61	1.21	1.26
	O_2 + CO	1.86	2.01	1.74	1.69
$Ag_xAu_{3-x}O$	O_2	1.25	1.15	0.71	1.07
	CO	1.57	1.62	0.91	0.94
	$CO+O_2$	1.57	1.62	1.23	1.21

[a]Values in eV. [b]See structure B in Figure 1.

clusters are triangles whose plane is orthogonal to the oxide surface, see Figure 1A, because of a "metal-on-top" effect.[33] The energy differences among the various upward configurations are small, and the energy barrier for diffusion via rotation in the out-of-plane axis is less than 0.5 eV. After adsorption of CO or unbroken O_2 in the lowest-energy configurations the M_3 triangle is still orthogonal to the oxide surface, see Figure 1B,E. Charge transfer from the surface is present but not crucial (see Supporting Information) and the main effect of the support is to provide an electrostatic field that changes substantially the energy landscape of the metal-cluster + ligands complex.[21] From Table 1, adsorption of the first O_2 molecule is exothermic by more than 1 eV, and the adsorption mode is parallel to one of the trimer edges, see Figure 1B.[34] On the contrary, for the second O_2 molecule there is basically no enthalpy gain for gold-rich clusters, whereas for silver-rich ones this amounts to 0.43 eV, at most, which hardly compensates for the loss of entropic contributions in standard conditions (about 0.5 eV for free O_2). In this case we thus do not find cooperative synergic effects on adsorption as in the gas-phase.[35] A further, substantial energy gain of 0.5−1.3 eV is obtained in breaking O_2 into two O atoms (we recall that this gain is not obtained for gas-phase trimers[18,21]). The energy barriers of the corresponding O_2 dissociation mechanisms (Figure 1B→C) are reported in Table 2 together with the associated enthalpy changes. It can be noticed that, despite the significant enthalpy gain, the barriers are quite large, so that this process is not

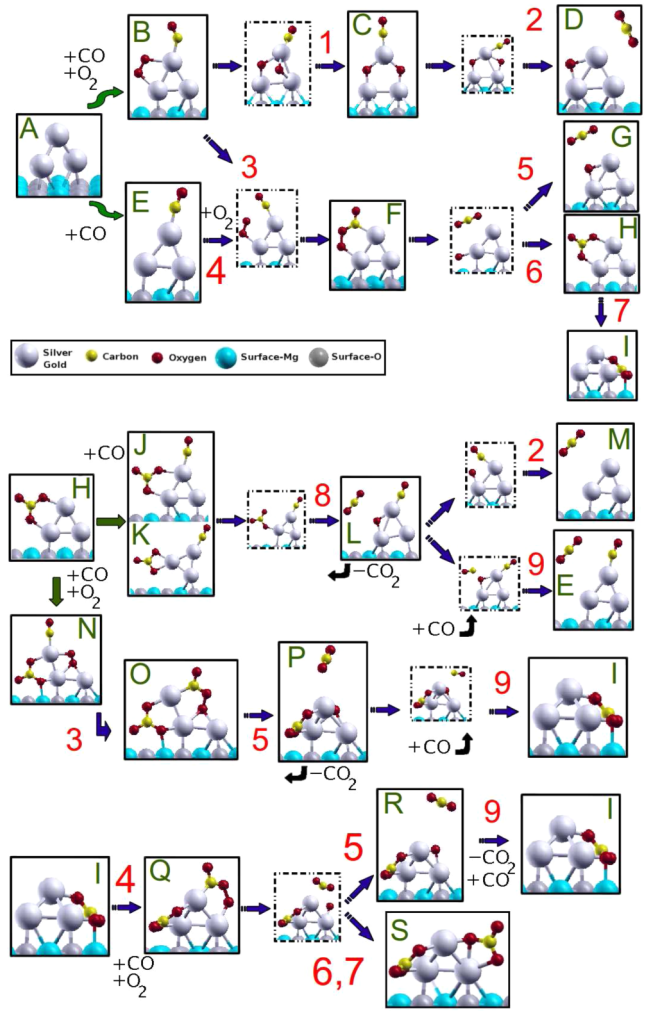

Figure 1. Main mechanisms found leading to CO oxidation. Local minima are enclosed by continuous lines and transition states by dashed lines.

Table 2. Energy Barriers[a] for O_2 Breaking on Ag_xAu_{3-x} Clusters[b]

Ag_0Au_3	Ag_1Au_2	Ag_2Au_1	Ag_3Au_0
2.17 (−1.26)	2.47 (−0.93)	1.91 (−0.56)	1.83 (−0.46)

[a]Enthalpy changes in parentheses. [b]Values in eV.

efficient in catalytic terms. The preferential site for CO is on top of the metal atom not in contact with the surface. Co-adsorption of two CO molecules is energetically favored by 0.45 eV at most, which is hardly sufficient to stabilize it in standard conditions when entropic contributions of free CO are taken into account (about 0.5 eV), again at variance with gas-phase cooperative synergic effects.[35]

The values in Table 1 show the greater affinity of Au-rich and Ag-rich clusters for CO and O_2, respectively, in tune with observation on gas-phase pure and alloyed clusters.[8−10] Co-adorption of CO and O_2 introduces a further interesting difference. Whereas for Au_3 and Ag_3 adsorption of only one CO or one O_2 molecule is thermodynamically favored in ambient conditions, for mixed Ag_xAu_{3-x} (x = 1,2) clusters simultaneously adsorbing one CO and one O_2 molecule maximizes the gain in enthalpy and is thermodynamically favorable even when

dx.doi.org/10.1021/cs300275v | ACS Catal. 2012, 2, 1860−1864

Table 3. Reaction Energy Barriers[a] for Selected Steps Leading to the Formation of CO_2(g)[b]

initial	final	mechanism	Ag_0Au_3	Ag_1Au_2	Ag_2Au_1	Ag_3Au_0
B	C	1 (LH)	0.83 (−0.77)	1.19 (−0.47)	1.20 (−0.37)	1.07 (−0.25)
C	D	2 (LH)	0.12 (−1.35)	0.20 (−1.35)	0.14 (−1.97)	0.05 (−2.13)
B	F	3 (LH)	0.38 (+0.11)	0.13 (+0.11)	0.09 (+0.08)	0.21 (−0.04)
E	F	4 (ER)	0.00 (−0.53)	0.00 (−0.77)	0.00 (−0.84)	0.00 (−0.95)
F	G	5 (LH)	0.71 (−2.23)	0.52 (−1.93)	0.30 (−2.43)	0.32 (−2.34)
F	H	6 (LH)	0.50 (−2.78)	0.52 (−3.00)	0.30 (−3.43)	0.32 (−3.37)
H	I	7 (LH)	0.30 (+0.27)		0.00 (−0.08)	0.00 (−0.20)
J	L	8 (LH)	0.36 (−0.17)	0.67 (+0.51)	0.71 (+0.71)	0.65 (+0.65)
L	M	2 (LH)	1.09 (−0.98)	0.89 (−1.11)	0.74 (−1.52)	0.67(−1.52)
L	E	9 (ER)	0.21 (−2.18)	0.20 (−2.28)		
N	O	3 (LH)	0.05 (−1.02)		0.05 (−0.77)	0.01 (−0.81)
O	P	5 (LH)	0.30 (−2.12)		0.29 (−2.89)	0.31 (−2.60)
P	I	9 (ER)	0.15 (−2.26)		0.18 (−2.27)	0.15 (−2.47)
I	Q	4 (ER)			0.05 (−1.40)	0.05 (−1.37)
Q	R	5 (LH)			0.37 (−2.80)	0.29 (−2.66)
Q	S	6−7 (LH)			0.37 (−2.73)	0.29 (−3.01)
R	H	9 (ER)			0.10 (−2.34)	0.11 (−2.50)

[a]Values in eV. Enthalpy change in parentheses. [b]See Figure 1 for the labels and an illustration of each structure/mechanism.

entropic contributions are included. The resulting $Ag_xAu_{3-x}O_2CO$ (x = 1,2) clusters are saturated.

Starting from M_3O_2CO complexes, two main routes[36] can lead to CO oxidation: (i) O_2 breaking followed by the reaction of an O atom with CO, or (ii) the direct interaction of adsorbed O_2 with (adsorbed or free) CO (active also for Pt clusters[37]). Both paths were found in the present simulations, the latter occurring according to a Langmuir−Hinshelwood mechanism when adsorption energies were favorable or to an Eley−Rideal one in the opposite case. The energetics of each case are reported in Table 3 and illustrated in Figure 1, which summarizes the results on reaction energy barriers. Route (i) presents larger energy barriers, even though, once O_2 is broken, CO_2 is immediately formed. In contrast, route (ii) leads to the formation of a M_3OOCO intermediate (Figure 1F)[24,38] (also observed in the gas-phase[28]), which can then either dissociate into M_3O + CO_2(g) or evolve into a very stable carbonate (CO_3) adduct, corresponding to the lowest-energy local minimum of these $Ag_xAu_{3-x}O_2CO$ complexes. The energy barriers are much lower with respect to route (i) so that this is the kinetically and thermodynamically preferred route.

Because of the high stability of the carbonate complex there is an energy penalty to break it into M_3O and CO_2(g). However, M_3CO_3 can take an additional CO (but no additional O_2) with an energy gain ranging from ≈0.5 eV (Ag-rich regime) to ≈1.0 eV (Au-rich regime). For Au_3 this weakens the M_3-CO_3 bond and lowers the energy barrier for removal of CO_2(g) (see Figure 1J→L and Table 3). The Au_3O complex so generated can adsorb additional molecules. In Table 1 the values for CO, O_2, and CO + O_2 absorption energies are given for each composition. For Au-rich complexes, the absorption of a CO molecule is energetically favorable, but the successive reaction with the adsorbed O atom to form CO_2 (mechanism 2) presents significant energy barriers, as shown in Table 3 (the $Ag_xAu_{3-x}O$ complexes are less efficient CO oxidation catalysts than Ag_xAu_{3-x} ones because of a stronger interaction with the O atom). In these conditions, an Eley−Rideal mechanism becomes favored. In Table 3 the reaction energy barriers for the reaction: CO(g) + OM_3CO→OM_3 + CO_2(g) via this mechanism are reported (mechanism 9) and are very low.

For Ag-rich compositions the energy difference of 0.65−0.71 eV (see Figure 1J,L and Table 3) for disaggregating the CO_3M_3CO complex slightly disfavors this process (even considering the gain in CO_2 free energy), and the reaction proceeds along a different route, in which the support plays an important role. The M_3CO_3 complex (Figure 1H) can in fact isomerize so that the carbonate directly interacts with the oxide surface (Figure 1I). This then absorbs CO and successively O_2 (Eley−Rideal mechanism) to produce a complex (Figure 1Q) which can then either disaggregate into OM_3CO_3 + CO_2(g) or tranform into a double carbonate complex (Figure 1S). If an OM_3CO_3 complex is generated (Figure 1R), this can interact with CO from the gas phase in an Eley−Rideal mechanism to produce another CO_2(g) and regenerate M_3CO_3 (Figure 1I). As apparent from Figure 1, this complex can also be produced via a different path in which upright M_3CO_3 (Figure 1H) absorbs CO and O_2 to give an intermediate (Figure 1O) which easily disaggregates into OM_3CO_3 + CO_2(g). The reaction of the bridged oxygen atom in OM_3CO_3 (Figure 1P) with gas phase CO then gives the M_3CO_3 complex (Figure 1I). A point which is important to stress is that for Ag_3 the inert double carbonate complex (Figure 1S) is energetically favored by 0.35 eV, so that the reaction may get stuck depending on the experimental conditions, whereas for Ag_2Au the path Figure 1Q→R is favored by about 0.1 eV. The difference between Ag_3 and Ag_2Au is due to the smaller oxygen affinity of Au (it is the carbonate on the Au side which disaggregates). In short, for Ag-rich compositions at variance with Au_3 the direct ligand interaction with the MgO support[22] plays a significant role, in tune with previous suggestions on other oxides[17,18] or larger particles.[38] Note that on MgO(100) effects such as ligand spillover from the support are not important. Figure 2 compares the sequence of local minima for CO oxidation on Au_3 and Ag-rich clusters.

A crucial feature of a catalyst is its stability in the given reaction conditions. To check this aspect of $(Ag-Au)_3$ supported trimers, the fragmentation energies of $Ag_xAu_{3-x}O_nCO_m$ complexes were determined. In Table 4 and Figure 3, the energy differences between the intact and the broken complexes are shown for six different cases: Ag_xAu_{3-x}, $Ag_xAu_{3-x}CO$, $Ag_xAu_{3-x}O_2$ (two different ways of breaking),

dx.doi.org/10.1021/cs300275v | ACS Catal. 2012, 2, 1860−1864

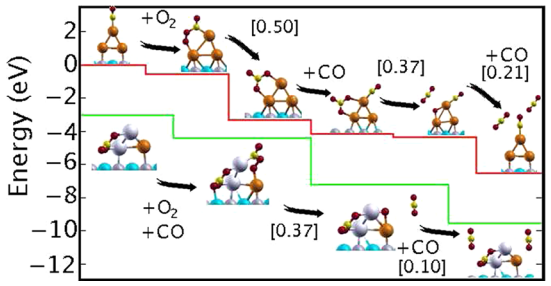

Figure 2. CO oxidation local minima steps for Ag_2Au(green) and Au_3(red). The Ag_2Au data are shifted by −3 eV for clarity. Reaction energy barriers are reported within square brackets.

Table 4. Minimum Energy Required to Break $Ag_xAu_{3-x}O_nCO_m$ Complexes into Smaller Pieces[a]

	Ag_0Au_3	Ag_1Au_2	Ag_2Au_1	Ag_3Au_0
a	0.64	0.77	0.69	0.68
b	0.64	0.67	0.83	1.10
c	2.22	1.50	1.63	1.63
d	0.58	0.87	0.99	0.96
e	2.04	1.86	2.31	1.89
f	0.07	0.37	0.71	0.85

[a]The configurations are shown in Figure 3. Values in eV.

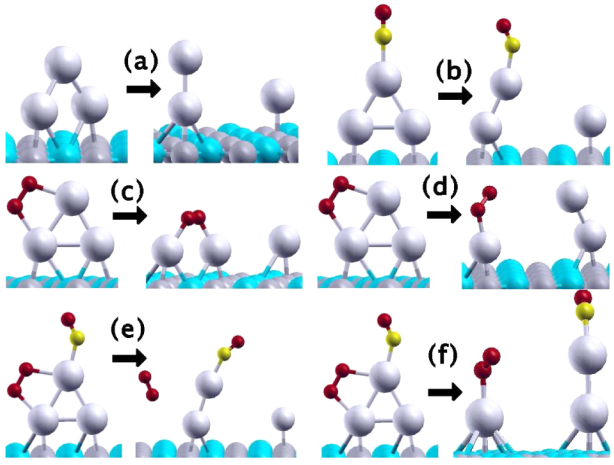

Figure 3. Breaking of three different $Ag_xAu_{3-x}O_nCO_m$ complexes. The atomic labels are the same as in Figure 1. Some structural differences exist depending on the exact composition of the complex.

and $Ag_xAu_{3-x}O_2CO$. Comparison of fragmentation paths (a) and (b) shows that CO adsorption increases the stability of silver-rich clusters. This pattern is also found when only O_2 is adsorbed (cases c and d), with the exception of Au_3. For the last 2 fragmentation paths, (e) and (f), when both O_2 and CO are adsorbed, silver-rich clusters are found to be still reasonably stable, whereas Au_3 and Ag_1Au_2 can break more easily than in the case of bare clusters in agreement with experiment.[39] We conclude that Au-rich trimers should have a shorter lifetime under a CO/O_2 atmosphere, which undermines their usefulness as candidates for the reaction under study.

Clearly, disgregation is one deactivation mechanism, diffusion leading to ripening and sintering being a different one. Under this viewpoint the regular MgO(100) surface shows limits as a support model, since, as mentioned earlier, the energy barriers for diffusion of the bare clusters are small. It can be noted in passing that pathways (c) and (e) are destabilized by the low adhesion of O_2 onto metal dimers. These barriers do increase after ligand adsorption especially for Ag-rich clusters (the effect of the interface is beneficial under this point of view) but to establish whether this is sufficient to prevent catalyst deactivation one should study the complex interplay between bare cluster and reactive complex diffusion under reaction conditions. Surface defects which trap and immobilize the clusters are probably needed to prevent this phenomenon and will be the subject of future work.

In summary, in this work the catalytic properties of Ag_xAu_{3-x}/MgO(100) clusters in CO oxidation were studied via a thorough DFT sampling of the PES of the metal-cluster + substrate + ligands systems.

Four main general conclusions can be drawn from this analysis.

First, even such a simple reaction as CO oxidation, led by a strong thermodynamic driving force and involving a limited number of chemical species, can occur through a variety of different mechanisms (some of them novel), ranging from CO-assisted O_2 breaking and successive CO reaction with a bridged oxygen species to the formation and successive decomposition of a carbonate (or a double carbonate) adduct, occurring via both Langmuir−Hinshelwood or Eley−Rideal mechanisms and with the assistance of the oxide surface or not.

Second, coverage effects (although often overlooked) are fundamental in determining the actual reaction paths in the given conditions. The catalytic active species in the cases here investigated are never bare metal clusters, but rather "catalytic complexes"[40,41] (the carbonate adduct of Figure 1I for Ag-rich compositions or the CO-doped cluster of Figure 1E for Au_3) which are formed under reaction conditions and which represent the heterogeneous catalysis analogue of the transition metal complexes utilized in homogeneous catalysis.

Third, the effect of alloying can be beneficial even though difficult to predict because of its highly nonlinear and many-body character, which is an intrinsic feature of subnanometer cluster energetics. In the present case Ag_2Au turns out to be a better CO oxidation catalyst than Ag_3 as it is able to coabsorb CO and O_2 in the first step of the reaction and to avoid getting stuck into unreactive intermediates at a later stage, because of the interplay of CO and O_2 affinity by Ag and Au, respectively.

Fourth, an analysis of the stability of these complexes with respect to fragmentation shows that Au-rich complexes are prone to breaking after coadsorption of CO and O_2 (in agreement with experiment), whereas alloying with silver significantly increases the cluster stability. We thus finally propose Ag_2Au_1 as the best candidate catalyst.

We believe that the present analysis offers interesting perspectives in the understanding and exploitation of heterogeneous subnanocatalysts while pointing to the need of efficient algorithms for structural exploration and sampling to achieve a predictive computational science.

■ ASSOCIATED CONTENT

Supporting Information

Computational details, representative charge and spin analysis and structures of M_3, M_3O_2, M_3O_2CO, and $Ag_3(CO_2)_2$ supported clusters. This information is available free of charge via the Internet at http://pubs.acs.org.

■ AUTHOR INFORMATION

Corresponding Author

*E-mail: alessandro.fortunelli@cnr.it.

Funding

Financial support from the ERC-AG SEPON project is gratefully acknowledged. This research used resources of the Oak Ridge Leadership Computing Facility, located in the National Center for Computational Sciences at Oak Ridge National Laboratory, which is supported by the Office of Science of the Department of Energy under Contract DE-AC05-00OR22725. S.V. thankfully acknowledges the support by the U.S. Department of Energy, BES Materials Sciences and Engineering Division, under Contract DE-AC-02-06CH11357 with UChicago Argonne, LLC, operator of Argonne National Laboratory.

Notes

The authors declare no competing financial interest.

■ ACKNOWLEDGMENTS

Part of the calculations were performed at the CASPUR supercomputing center (Italy) within the TheoNanoCat project. Networking from the MP0903 COST action is also acknowledged.

■ REFERENCES

(1) Twigg, M. V. *Appl. Catal., B* **2007**, *70*, 2.
(2) Royer, S.; Duprez, D. *ChemCatChem* **2011**, *3*, 24.
(3) Haruta, M.; Kobayashi, T.; Sano, H.; Yamada, M. *Chem. Lett.* **1987**, *16*, 405−409.
(4) Bond, G. C.; Louis, C.; Thomson, D. T. *Catalysis by gold*; Imperial College Press: London, U.K., 2006.
(5) Min, B. K.; Friend, C. M. *Chem. Rev.* **2007**, *107*, 2709.
(6) Frondelius, P.; Häkkinen, H.; Honkala, K. *Phys. Rev. B* **2007**, *76*, 073406.
(7) Chretien, S.; Buratto, S. K.; Metiu, H. *Curr. Opin. Solid State Mater. Sci.* **2007**, *11*, 62.
(8) Joshi, A. M.; Delgass, W. N.; Thomson, K. T. *J. Phys. Chem. B* **2006**, *110*, 23373−23387.
(9) Joshi, A. M.; Tucker, M. H.; Delgass, W. N.; Thomson, K. T. *J. Chem. Phys.* **2006**, *125*, 194707.
(10) Popolan, D. M.; Nößler, M.; Mitrić, R.; Bernhardt, T. M.; Holger; Bonačić-Koutecký, V. *Phys. Chem. Chem. Phys.* **2010**, *12*, 7865−7873.
(11) Remediakis, I. N.; Lopez, N.; Nørskov, J. K. *Angew. Chem.* **2005**, *117*, 1858−1860.
(12) Choudhary, T.; Goodman, D. *Top. Catal.* **2002**, *21*, 25−34.
(13) Zhang, C.; Yoon, B.; Landman, U. *J. Am. Chem. Soc.* **2007**, *129*, 2228−2229.
(14) Herzinga, A. A.; Kiely, C. J.; Carley, A. F.; Landon, P.; Hutchings, G. J. *Science* **2008**, *321*, 1331−1335.
(15) Heiz, U.; Sanchez, A.; Abbet, S.; Schneider, W.-D. *J. Am. Chem. Soc.* **1999**, *121*, 3214−3217.
(16) Yoon, B.; Hakkinen, H.; Landman, U.; Worz, A. S.; Antonietti, J. M.; Abbet, S.; Judai, K.; Heiz, U. *Science* **2005**, *307*, 403−407.
(17) Lee, S.; Molina, L.; López, M.; Alonso, J.; Hammer, B.; Lee, B.; Seifert, S.; Winans, R.; Elam, J.; Pellin, M.; Vajda, S. *Ang. Chem., Int. Ed.* **2009**, *48*, 1467−1471.
(18) Lei, Y.; Mehmood, F.; Lee, S.; Greeley, J. P.; Lee, B.; Seifert, S.; Winans, R. E.; Elam, J. W.; Meyer, R. J.; Redfern, P. C.; Teschner, D.; Schl.ogl, R.; Pellin, M. J.; Curtiss, L. A.; Vajda, S. *Science* **2010**, *328*, 224.
(19) Sinfelt, J. H. *Acc. Chem. Res.* **1977**, *10*, 15−20.
(20) Bazin, D. *Macromol. Res.* **2006**, *14*, 230−234.
(21) Negreiros, F. R.; Aprá, E.; Barcaro, G.; Sementa, L.; Vajda, S.; Fortunelli, A. *Nanoscale* **2012**, *4*, 1208.
(22) Lee, S.; Fan, C.; Wu, T.; Anderson, S. L. *J. Chem. Phys.* **2005**, *123*, 124710.
(23) Amft, M.; Skorodumova, N. V. *Phys. Rev. B* **2010**, *81*, 195443.
(24) Chang, C. M.; Cheng, C.; Wei, C. M. *J. Chem. Phys.* **2008**, *128*, 124710.
(25) Inderwildi, O.; Jenkins, S.; King, D. *Surf. Sci.* **2007**, *601*, L103−L108.
(26) Bernhardt, T. M.; Hagen, J.; Lang, S. M.; Popolan, D. M.; Socaciu-Siebert, L. D.; Wöste, L. *J. Phys. Chem. A* **2009**, *113*, 2724−2733.
(27) Bernhardt, T. M.; Socaciu-Siebert, L. D.; Hagen, J.; Wöste, L. *Appl. Catal., A* **2005**, *291*, 170−178.
(28) Socaciu, L. D.; Hagen, J.; Roux, J. L.; Popolan, D.; Bernhardt, T. M.; Wöste, L.; Vajda, S. *J. Chem. Phys.* **2004**, *120*, 2078−2081.
(29) Sandoval, A.; Aguilar, A.; Louis, C.; Traverse, A.; Zanella, R. *J. Catal.* **2011**, *281*, 40−49.
(30) Moskaleva, L. V.; Zielasek, V.; Kluener, T.; Neyman, K. M.; Baeumer, M. *Chem. Phys. Lett.* **2012**, *525−26*, 87−91.
(31) Perdew, J.; Burke, K.; Ernzerhof, M. *Phys. Rev. Lett.* **1996**, *77*, 3865.
(32) Giannozzi, P.; et al. *J. Phys.: Condens. Matter* **2009**, *21*, 395502 (19pp).
(33) Barcaro, G.; Fortunelli, A. *J. Chem. Theory Comput.* **2005**, *1*, 972.
(34) Klacar, S.; Hellman, A.; Panas, I.; Grönbeck, H. *J. Phys. Chem. C* **2010**, *114*, 12610−12617.
(35) Hagen, J.; Socaciu, L. D.; Le Roux, J.; Popolan, D.; Bernhardt, T. M.; Wöste, L.; Mitrić, R.; Noack, H.; Bonačić-Koutecký, V. *J. Am. Chem. Soc.* **2004**, *126*, 3442−3443.
(36) Chen, Y.; Crawford, P.; Hu, P. *Catal. Lett.* **2007**, *119*, 21−28.
(37) Allian, A. D.; Takanabe, K.; Fujdala, K. L.; Hao, X.; Truex, T. J.; Cai, J.; Buda, C.; Neurock, M.; Iglesia, E. *J. Am. Chem. Soc.* **2011**, *133*, 4498−4517.
(38) Molina, L. M.; Hammer, B. *Phys. Rev. B* **2004**, *69*, 155424.
(39) Saint-Lager, M. C.; Laoufi, I.; Robach, O.; Garaudee, S.; Dolle, P. *Faraday Discuss.* **2011**, *152*, 253.
(40) Mager-Maury, C.; Bonnard, G.; Chizallet, C.; Sautet, P.; Raybaud, P. *ChemCatChem* **2011**, *3*, 200−207.
(41) Beret, E. C.; Ghiringhelli, L. M.; Scheffler, M. *Faraday Discuss.* **2011**, *152*, 153−167.